

Neutron emission from electromagnetic dissociation of Pb nuclei at $\sqrt{s_{NN}} = 2.76$ TeV measured with the ALICE ZDC

P. Cortese^{1,a} for the ALICE Collaboration^b

Abstract. The ALICE Zero Degree Calorimeter system (ZDC) is composed of two identical sets of calorimeters, placed at opposite sides with respect to the interaction point, 114 meters away from it, complemented by two small forward electromagnetic calorimeters (ZEM). Each set of detectors consists of a neutron (ZN) and a proton (ZP) ZDC. They are placed at zero degrees with respect to the LHC axis and allow to detect particles emitted close to beam direction, in particular neutrons and protons emerging from hadronic heavy-ion collisions (spectator nucleons) and those emitted from electromagnetic processes. For neutrons emitted by these two processes, the ZN calorimeters have nearly 100% acceptance.

During the $\sqrt{s_{NN}} = 2.76$ TeV Pb-Pb data-taking, the ALICE Collaboration studied forward neutron emission with a dedicated trigger, requiring a minimum energy deposition in at least one of the two ZN. By exploiting also the information of the two ZEM calorimeters it has been possible to separate the contributions of electromagnetic and hadronic processes and to study single neutron vs. multiple neutron emission.

The measured cross sections of single and mutual electromagnetic dissociation of Pb nuclei at $\sqrt{s_{NN}} = 2.76$ TeV, with neutron emission, are $\sigma_{\text{single EMD}} = 187.4 \pm 0.2$ (stat.) $^{+13.2}_{-11.2}$ (syst.) b and $\sigma_{\text{mutual EMD}} = 5.7 \pm 0.1$ (stat.) ± 0.4 (syst.) b, respectively [1]. This is the first measurement of electromagnetic dissociation of ^{208}Pb nuclei at the LHC energies, allowing a test of electromagnetic dissociation theory in a new energy regime. The experimental results are compared to the predictions from a relativistic electromagnetic dissociation model.

1 Introduction

When two interacting nuclei collide at an impact parameter larger than the sum of the nuclear radii the interaction can only be electromagnetic. The electromagnetic field of one of the two ions is perceived by the other ion as a flux of virtual photons. This can be approximated through the equivalent photon method, first proposed by Fermi [2] in order to treat the moving electromagnetic field of a charged particle, and later extended by Weizsäcker and Williams to collisions of ultra-relativistic electrons and protons with nuclei [3, 4]. As the beam energy increases, the photon spectrum hardens and the flux is enhanced, due to the Lorentz contraction of the Coulomb field. Moreover, the photon flux is proportional to Z^2 , where Z is the charge number of the emitting nucleus. Therefore, the electromagnetic interactions become dominant in ultra-relativistic collisions of heavy-ions with respect to

^ae-mail: cortese@to.infn.it

^bFull author list is given in Appendix A

hadronic processes. In particular the bound-free pair production and the electromagnetic dissociation (EMD), have attracted special attention in the last years, since they strongly limit the beam lifetime in heavy-ion colliders [5].

Theoretical models [6] predict that the electromagnetic dissociation of colliding ^{208}Pb nuclei occurs mainly through the excitation and subsequent decay of the Giant Dipole Resonance (GDR) ($\sim 60\%$ of EMD events at the LHC) and therefore via emission of one or two neutrons. This can be exploited to measure the luminosity at heavy-ion colliders by detecting forward neutrons [7] using the Zero Degree Calorimeters (ZDCs) as is done in the ALICE experiment [8] at the Large Hadron Collider (LHC). The ZDCs are ideally suited to tag EMD interactions, since the resulting neutrons from the GDR decay are emitted very close to the beam rapidity and are the most abundant particles produced in these processes.

The data were collected using the neutron ZDCs (ZNA and ZNC), located 114 m away from the Interaction Point (IP) at the so-called A and C sides of the ALICE detector. Each ZN is placed at zero degree with respect to the LHC beam axis and is used to detect neutral particles at pseudo-rapidities $|\eta| > 8.7$. The neutron and proton calorimeters are based on the detection of Cherenkov light produced in quartz fibers by the hadronic showers. Each detector is readout by five photomultipliers. Half of the fibers go to a “common” photomultiplier, the rest of the fibers are grouped to provide a coarse transverse segmentation of the calorimeter into four towers. For the present analysis two small forward electromagnetic calorimeters (ZEM1 and ZEM2), placed on the A side at 7.35 m from the IP ($4.8 \leq \eta \leq 5.7$), are also used to tag hadronic interactions.

The experimental results are compared to theoretical predictions of the Relativistic Electromagnetic DIssociation (RELDIS) model [6], which is designed to describe electromagnetic interactions between ultra-relativistic nuclei including single and double virtual photon absorption, excitation of giant resonances, intra-nuclear cascades of produced hadrons and statistical decay of excited residual nuclei. Above the GDR energy region, photon-induced reactions become more complicated leading to multiple (>3) emission of neutrons [9]. RELDIS accurately reproduces this experimental observation and also predicts further increase of the mean number of neutrons and of the width of their multiplicity distribution as photon energy increases [10]. Calculations based on this model provide a good description of neutron emission in electromagnetic dissociation of Pb ions at the CERN SPS [11] and of Au ions at the Relativistic Heavy Ion Collider (RHIC) [12].

2 Experimental results

During the $\sqrt{s_{\text{NN}}} = 2.76$ TeV Pb-Pb data taking in 2010, a dedicated trigger was setup, during a limited period of time, to study in detail EMD dissociation. In this special run only the ZDCs and ZEM were readout. The trigger was set to tag neutrons emitted in EMD as well as hadronic interactions (see Figure 1), requiring a minimum energy deposition in at least one of the two ZNs (ZNA OR ZNC). A total of $\sim 3 \times 10^6$ events were collected. The energy thresholds were ~ 450 GeV for ZNA and ~ 500 GeV for ZNC and were placed approximately three standard deviations below the energy deposition of a 1.38 TeV neutron. Such a low threshold was achieved using custom differential discriminators, designed and realized following the idea of [13] that allows to reach a good triggering performance even in presence of oscillations of the signal baseline. We also achieved a good immunity from the photomultiplier noise exploiting the redundancy in the sampling that is present in the calorimeter design.

Following a common convention we define as single EMD an electromagnetic process where at least one neutron (1n) is emitted by a given Pb nucleus regardless of the fate of the other nucleus. Given this definition, Mutual EMD events, where at least 1n is emitted by both Pb nuclei following a

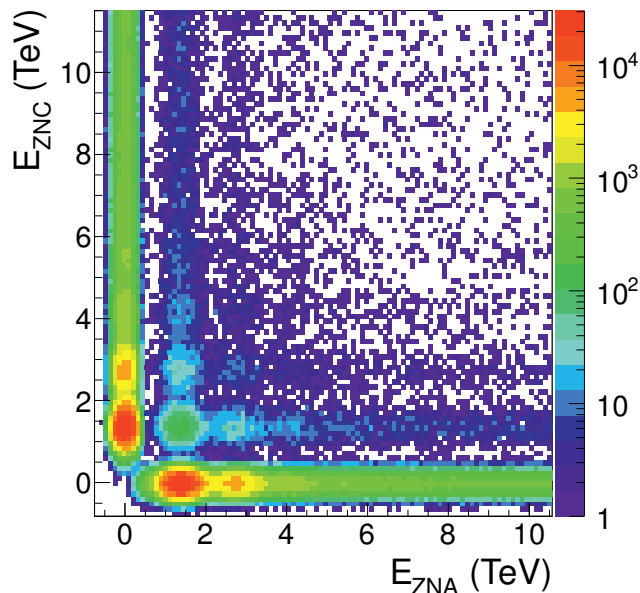


Figure 1. Energy deposition in ZNC versus ZNA for single EMD plus hadronic events. The one neutron signal is at 1.38 TeV. The events where at least one neutron is detected by both ZNs are associated to mutual EMD and hadronic processes. The depletion of events in the region where the ZNA and ZNC energy deposition is close to 0 TeV is related to the (ZNA OR ZNC) trigger threshold [1].

double photon exchange, are a subsample of single EMD events. Mutual EMD events and hadronic events were selected offline requiring an energy deposit above the energy threshold in both ZNs.

In the 2010 Pb-Pb data taking the neutron calorimeters were used as the ALICE luminometer, providing different logical combinations of signals (ZDC triggers), among which the trigger (ZNA OR ZNC) used for the EMD study. During a van der Meer (vdM) scan of the beams [14], a cross section $\sigma_{ZNA\ OR\ ZNC}^{vdM} = 371.4 \pm 0.6$ (stat.) $^{+24}_{-19}$ (syst.) b was measured for the (ZNA OR ZNC) trigger, tagging single EMD plus hadronic interactions. The systematic error of $-5.2\% + 6.4\%$ can be decomposed as follows: 4.3% uncertainty coming from the vdM scan analysis [15], dominated by the calibration of the distance scale during the scan; $-3\% + 4.7\%$ uncertainty coming from the measurement of the beam intensity, dominated by the beam current transformers scale [16] and by the non-colliding (ghost) charge fraction in the LHC beams [17, 18]. The beam-gas contribution ($\sim 2.5\%$) is taken into account in the vdM fit and subtracted.

The energy spectrum for the ZNA is shown in Figure 2, for events in which there is a signal in at least one of the two ZNs or for events in which ZNA is fired. The selection of events with signal in ZNA is performed offline using the timing information provided by a TDC (Time to Digital Converter). This provides a sharper cut with respect to a selection based on energy deposition since it is using discriminated signals obtained with the above mentioned differential discriminators that are insensitive to the oscillations of the signal baseline. The timing information is also useful to reject the very small contribution from collisions between the main and satellite bunches. In Fig. 2 a pedestal peak centered at $E = 0$ is visible, which corresponds to events with no signal detected by the ZNA and the trigger (ZNA OR ZNC) fired by the ZNC. As can be inferred from this figure, the TDC selection rejects only events in the pedestal region. The width of the pedestal peak is related to the noise of electronic modules. In the energy spectrum a pronounced 1n peak at 1.38 TeV is present, but also 2n, 3n, 4n... peaks are clearly identified. The requirement of a signal in the TDC for the ZNA and the ZNC, respectively, allows to calculate two different estimates of the number of events from single EMD plus hadronic processes, i.e. the number of events with a signal in ZNA or ZNC, respectively.

The average of the two results is then computed (the difference between the response of the ZNA and the ZNC is about 0.1%). The contamination from beam-residual gas interactions could not be directly measured as was done in the vdM scan. However, we obtained an estimation from the observed rates with circulating beams, before they are brought into collisions. It is of the order of 2.5% and is corrected for.

A second event selection requires a signal in one of the ZNs and nothing in the other one. In this way hadronic events, which mostly lead to the disintegration of both colliding nuclei, are rejected. In this case, the mutual EMD events are also removed from the spectrum and therefore the selected process is the single EMD minus the mutual EMD. The energy spectrum is shown in Figure 3 together with the fit obtained by summing four Gaussians. The curve for the 1n peak has three free parameters, while the following Gaussians describing the i^{th} peak have a constraint both on the mean value μ_{in} ($\mu_{in} = i \times \mu_{1n}$, where μ_{in} is the mean value for i^{th} neutron peak) and on the width σ_{in} ($\sigma_{in} = \sqrt{i \times (\sigma_{1n}^2 - \sigma_{ped}^2) + \sigma_{ped}^2}$, where σ_{in} is the width of the i^{th} neutron peak and σ_{ped} is the width of the pedestal peak that is obtained previously to the fit). The relative energy resolution σ_{1n}/μ_{1n} of the 1n peak at 1.38 TeV is 21% for the ZNA and 20% for the ZNC, in agreement with expectations from beam tests at the CERN SPS [19] extrapolated to LHC energies using Monte Carlo simulations, which take into account the different projectile energies, the momentum spectra of the emitted neutrons, the different operating conditions of the photomultipliers and the different noise contribution (pedestal). Similarly to the previous analysis we used the average of the ZNA and the ZNC cross sections, the difference of which is about 0.2%.

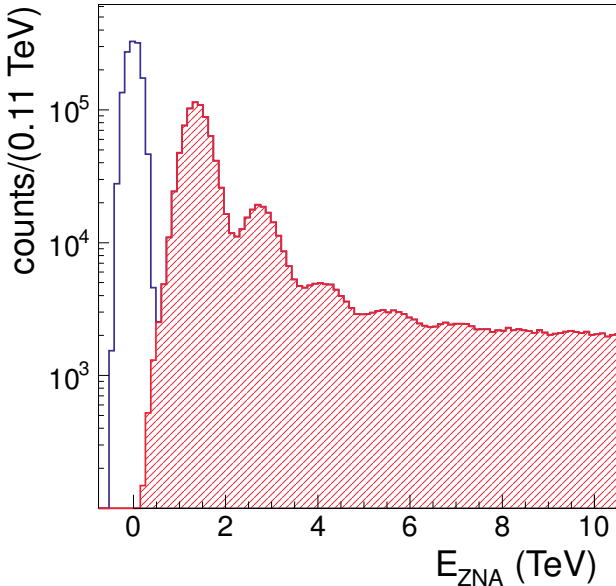


Figure 2. ZNA energy spectrum requiring signal over threshold in ZNA or ZNC superimposed to ZNA energy spectrum requiring signal in ZNA (shaded area). The first peak centered at $E = 0$ corresponds to pedestal events, where the trigger is fired by ZNC and no signal from neutron emission is detected by the ZNA (and therefore ZNA signal can be below threshold) [1].

The cross sections, listed in Table 1 (first two rows), are calculated using the cross section for having a signal either in ZNA or in ZNC, $\sigma_{ZNA\ OR\ ZNC}^{vdM}$, measured during the vdM scan: $\sigma_{proc} = \sigma_{ZNA\ OR\ ZNC}^{vdM} \times N_{proc}/N_{ZNA\ OR\ ZNC}$, where N_{proc} is the number of events in the sample of the selected process and $N_{ZNA\ OR\ ZNC}$ is the number of events collected with the same trigger as used to determine $\sigma_{ZNA\ OR\ ZNC}^{vdM}$. The calculated values are corrected for the ZN detection probability ($98.7\% \pm 0.04\%$ (stat.) $\pm 0.1\%$ (syst.)), estimated from a Monte Carlo simulation using RELDIS as event gen-

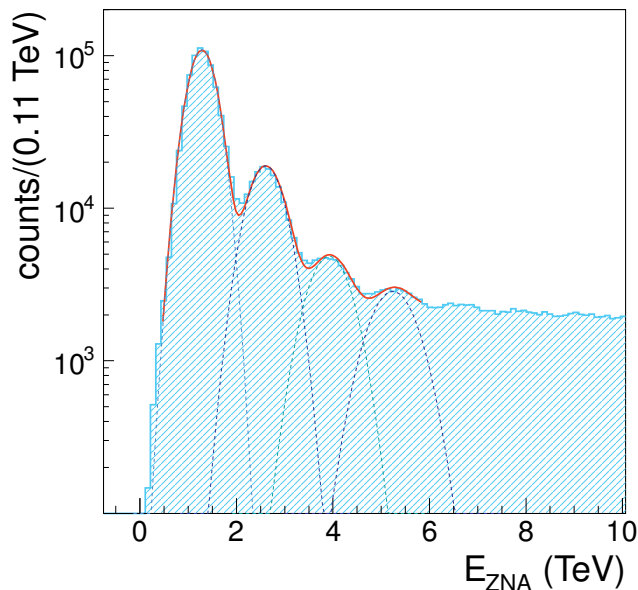


Figure 3. ZNA energy spectrum requiring signal over threshold in ZNA but not in ZNC, rejecting thus neutron emission on the opposite side. The dashed lines represent the single fits of the different peaks (1n, 2n,...), while the continuous line is the sum of all the contributions [1].

Table 1. Neutron emission cross sections at $\sqrt{s_{NN}} = 2.76$ TeV in Pb-Pb interactions (systematic errors are dominated by the vdM cross section errors). The predictions of the RELDIS model for $\sqrt{s_{NN}} = 2.76$ TeV Pb-Pb EMD interactions are also shown. Theoretical uncertainties are systematic and related to uncertainties in the total photoabsorption cross sections on Pb [1].

Physical Process	Cross section (barn)	RELDIS prediction (barn)
single EMD + hadronic	194.8 ± 0.3 stat. $^{+13.6}_{-11.5}$ syst.	192.9 ± 9.2
single EMD - mutual EMD	181.3 ± 0.3 stat. $^{+12.8}_{-10.9}$ syst.	179.7 ± 9.2
mutual EMD	5.7 ± 0.1 stat. ± 0.4 syst.	5.5 ± 0.6
hadronic	7.7 ± 0.1 stat. $^{+0.6}_{-0.5}$ syst.	7.7 ± 0.4
single EMD	187.4 ± 0.2 stat. $^{+13.2}_{-11.2}$ syst.	185.2 ± 9.2

erator. The systematic errors, dominated by the uncertainties of the cross sections measured during the vdM scan, take also into account the difference between the response of the ZNA and the ZNC (0.1-0.2%) and the uncertainty due to the estimate of beam-gas background ($\sim 1\%$). The centering of ZN calorimeters on the neutron spot was assured by the measurement of the centroid position, thanks to their transverse segmentation in four towers.

The agreement between data and RELDIS model predictions is remarkable (see Table 1). In calculations of the EMD cross sections various approximations of the total photoabsorption cross sections on lead are used, leading to 5% uncertainties in the predicted values [6]. These errors include the difference between RELDIS and other theoretical predictions [20].

A third event selection is performed to select mutual EMD and hadronic events requiring a minimum energy deposition in both ZNs. This selection rejects all beam-gas contributions. The ZEMs are used to disentangle between the two processes. By selecting events with no signal in any ZEM we

isolate the sample of EMD events, vice versa, by requiring a signal in at least one of the two ZEMs we identify hadronic processes as can be seen in Figure 4. The energy threshold for each ZEM is about 10 GeV.

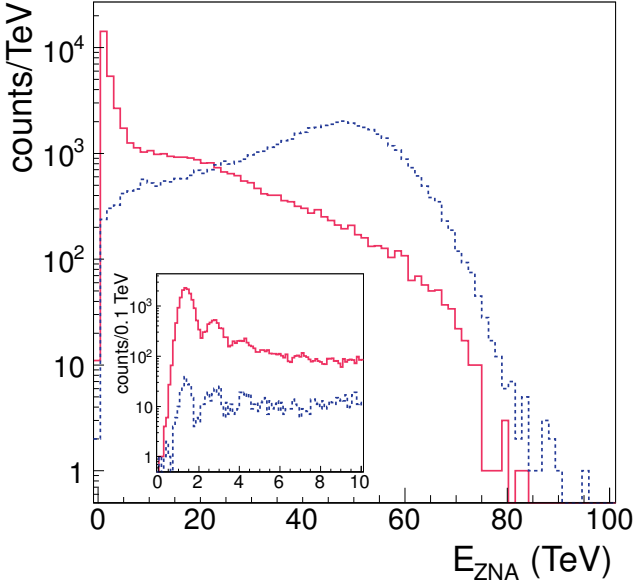


Figure 4. ZNA energy spectrum for mutual EMD (no signal in any ZEM, continuous line) and hadronic (a signal in at least one of the two ZEMs, dashed line) event selection. The insert shows an expanded view of the low energy region [1].

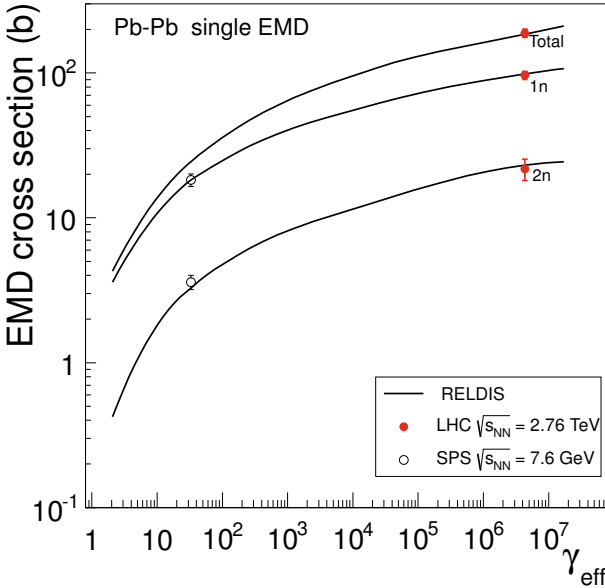


Figure 5. Total single EMD cross sections and partial EMD cross sections for emission of one and two neutrons as a function of the effective Lorentz factor γ_{eff} (the projectile Lorentz-factor in the rest frame of the collision partner). The filled symbols are ALICE data [1], while the open symbols represent the results obtained at the CERN SPS [11] at 30 GeV. The RELDIS predictions [11] for total, 1n and 2n EMD cross sections are shown as solid lines.

The cross sections for the mutual EMD and hadronic processes are calculated, as in the previous analysis, starting from $\sigma_{\text{ZNA OR ZNC}}^{\text{vdM}}$. However, given the fact that the ZEM calorimeters are not 100%

efficient in tagging hadronic interactions, these cross sections are biased by a small cross contamination and therefore we refer to them as “raw” cross sections. The ZEM trigger efficiencies for the mutual EMD event selection, i.e. the fraction of mutual EMD events with no signal in any ZEM, is $96.0\% \pm 0.1\%(\text{stat.}) \pm 0.6\%(\text{syst.})$, evaluated from simulation using RELDIS as event generator. The ZEM trigger efficiencies for the hadronic event selection, i.e. the the fraction of hadronic events with a signal in at least one of the two ZEMs, is $92.4\% \pm 0.3\%(\text{stat.}) \pm 1.0\%(\text{syst.})$, estimated using HI-JING [21] as event generator, combined with a simple fragmentation model [22]. Since the two event selections are mutually exclusive, the contamination of mutual EMD events in the hadronic sample and of hadronic events in the mutual EMD sample are $\sim 4\%$ and $\sim 7.6\%$ respectively.

The raw cross sections ($\sigma_{mEMD,raw}$, $\sigma_{hadr,raw}$) and the ZEM trigger efficiencies (ϵ_{mEMD} , ϵ_{hadr}) for the two processes are inserted in a system of equations with two variables, where the unknowns are the true mutual EMD and the true hadronic cross sections ($\sigma_{mEMD,true}$, $\sigma_{hadr,true}$), respectively.

$$\begin{cases} \sigma_{mEMD,raw} &= \epsilon_{mEMD} \cdot \sigma_{mEMD,true} + (1 - \epsilon_{hadr}) \cdot \sigma_{hadr,true} \\ \sigma_{hadr,raw} &= (1 - \epsilon_{mEMD}) \cdot \sigma_{mEMD,true} + \epsilon_{hadr} \cdot \sigma_{hadr,true} \end{cases}$$

The extracted values are corrected for the estimated ZN detection probability for mutual EMD ($95.7\% \pm 0.07\%(\text{stat.}) \pm 0.5\%(\text{syst.})$) and for hadronic ($97.0\% \pm 0.2\%(\text{stat.}) \pm 3\%(\text{syst.})$) events. The mutual EMD cross section is also corrected for background from accidental coincidences between uncorrelated single EMD interactions ($\sim 10\%$). The final cross section results are summarized and compared to the RELDIS predictions in Table 1 (third and fourth rows).

The single EMD cross section listed in Table 1 (last row) is estimated from previous measurements, taking an average of the (single EMD + hadronic) – hadronic and the (single EMD – mutual EMD) + mutual EMD cross sections.

For the single EMD minus mutual EMD event selection the measured fractions of 1n, 2n and 3n events with respect to the total number of events is estimated (Table 2). This data sample is particularly interesting because there is no contamination from hadronic interactions. The table contains also the relevant expectations for the ratios based on the calculations with the RELDIS model. The 1n and 2n emission channels give the main contribution (63%), confirming that EMD processes proceed predominantly via GDR excitation and subsequent decay by neutron emission. According to RELDIS, 3n emission is mostly induced by energetic (> 40 MeV) equivalent photons and frequently accompanied by emission of protons and pions. The measured 1n and 2n yields are much closer to RELDIS predictions compared to the 3n yields. This can be explained by the fact that RELDIS was already tuned by comparison with 1n and 2n data on photoabsorption on lead [6] and on EMD of 30 A GeV lead nuclei [11]. Unfortunately, the data on neutron emission induced by photons above 140 MeV are absent and, according to RELDIS, almost half of 3n events is due to such energetic photons. The theoretical uncertainty on RELDIS predictions listed in Table 2 are estimated by replacing its native photonuclear reaction model with the GNASH code [23]. The differences between the two predictions are used as an estimate of the uncertainties.

The measured ratio 2n/1n in single EMD ($22.5 \pm 0.5 \pm 0.9\%$) can be compared to the value of ($19.7 \pm 2.9\%$) reported for Pb-Pb collisions at 30 A GeV at the CERN SPS [11]. As predicted by RELDIS, the observed weak increase (around one standard deviation) of the 2n to 1n ratio with increasing collision energy is due to additional 2n events produced by more energetic equivalent photons at the LHC.

In Figure 5 we compare RELDIS predictions with ALICE [1] and SPS data [11]. Both data sets are successfully described by the model despite of six orders-of-magnitude span of the effective projectile Lorentz-factor γ_{eff} . A direct comparison to RHIC results is not straightforward since the structures of the nuclei are different. Since ^{208}Pb , used at the LHC, is a double magic nucleus, while ^{197}Au ,

Table 2. The neutron emission fractions for single EMD minus mutual EMD process in $\sqrt{s_{NN}} = 2.76$ TeV Pb-Pb interactions [1], defined as the number of events with a given neutron multiplicity (1n, 2n or 3n) divided by the total number of events (N_{tot}), together with the ratio of 2n and 1n events [1]. Theoretical uncertainties are systematic and related to the difference of the predictions of two photonuclear reaction models.

Ratio	Data(%)	RELDIS(%)
$1n/N_{tot}$	51.5 ± 0.4 stat. ± 0.2 syst.	54.2 ± 2.4
$2n/N_{tot}$	11.6 ± 0.3 stat. ± 0.5 syst.	12.7 ± 0.8
$3n/N_{tot}$	3.6 ± 0.2 stat. ± 0.2 syst.	5.4 ± 0.7
$2n/1n$	22.5 ± 0.5 stat. ± 0.9 syst.	23.5 ± 2.5

used at RHIC is not, the GDR position, its width as well as the neutron emission thresholds differ significantly.

3 Conclusions

In summary, a first measurement of electromagnetic dissociation in $\sqrt{s_{NN}} = 2.76$ TeV Pb-Pb collisions was performed at the LHC by detecting the emitted neutrons with the ALICE ZDCs [1] with an increased detail compared with previous measurements at colliders at lower energies [12]. In fact, in our case, both single and mutual electromagnetic dissociation cross sections were measured and the hadronic cross section was estimated at the same time. The measurement tests the theoretical predictions used for estimating beam losses. The RELDIS model predictions are in a very good agreement with the ALICE experimental results. The ALICE measurements establish experimentally the EMD cross section scale for the first time at LHC energy. Note that the ALICE ZDC detectors, calibrated through these results, provide the possibility of a direct absolute measurement of the LHC luminosity in Pb-Pb collisions.

References

- [1] K. Aamodt et al. (ALICE Collaboration), arXiv:1203.2436 [nucl-ex]. To be published in Physical Review Letters.
- [2] E. Fermi, Z. Phys. **29**, 315 (1924).
- [3] C.F. von Weizsäcker, Z. Phys. **88**, 612 (1934).
- [4] E.J. Williams, Phys. Rev. **45**, 729 (1934).
- [5] R. Bruce et al., Phys. Rev. ST Accel. Beams **12**, 071002 (2009).
- [6] I.A. Pshenichnov et al., Phys. Rev. C **64**, 024903 (2001); I.A. Pshenichnov, Phys. Part. Nucl. **42**, 215 (2011).
- [7] A.J. Baltz, C. Chasman, S.N. White, Nucl. Instr. and Methods in Phys. Research A **417**, 1 (1998).
- [8] K. Aamodt et al. (ALICE Collaboration), J. Instrum. **3**, S08002 (2008).
- [9] A. Lepretre et al., Nucl. Phys. A **390**, 221 (1982).
- [10] I.A. Pshenichnov et al., Phys. Rev. C **60**, 044901 (1999).
- [11] M.B. Golubeva et al., Phys. Rev. C **71**, 024905 (2005).
- [12] M. Chiu et al., Phys. Rev. Lett. **89**, 012302 (2002).
- [13] D. Brahy and E. Rossa, NIM **192** 359 (1982), CERN/SPS/81-11 (EBP).
- [14] S. van der Meer, CERN/ISR-PO/68-31 (1968).

- [15] K.Oyama for the ALICE Collaboration, Proceedings of the LHC Lumi Days 2012, to be published.
- [16] A. Alici et al., CERN-ATS-Note-2011-016 PERF (LHC BCN WG Note 2).
- [17] A. Jeff, Proceedings of the LHC Lumi Days 2012, to be published.
- [18] A. Alici et al., CERN-ATS-Note-2012-029 PERF (LHC BCN WG Note 4).
- [19] R. Arnaldi et al., Nucl. Instr. and Meth. A **564**, 235 (2006); N. De Marco et al., IEEE Trans. on Nucl. Science **54 No.3**, 567 (2007).
- [20] A.J. Baltz et al., Physics Reports **458** (2008); A.J. Baltz, S.N. White, private communication.
- [21] X.-N. Wang and M. Gyulassy, Phys. Rev. D **44**, 3501 (1991).
- [22] ALICE Zero Degree Calorimeter Technical Design Report, CERN/LHCC **99-5**, ALICE TDR 3 (1999), <https://edms.cern.ch/document/398933/1>.
- [23] M.B. Chadwick, P.G. Young, Acta Phys. Slov. **45**, 633 (1995).

A The ALICE Collaboration

B. Abelev⁶⁸, J. Adam³³, D. Adamová⁷³, A.M. Adare¹¹⁹, M.M. Aggarwal⁷⁷, G. Aglieri Rinella²⁹, A.G. Agocs⁶⁰, A. Agostinelli²¹, S. Aguilar Salazar⁵⁶, Z. Ahammed¹¹⁵, N. Ahmad¹³, A. Ahmad Masoodi¹³, S.U. Ahn^{63,36}, A. Akimov⁴⁶, D. Aleksandrov⁸⁸, B. Alessandro⁹⁴, R. Alfaro Molina⁵⁶, A. Alici^{97,9}, A. Alkin², E. Almaráz Avaña⁵⁶, J. Alme³¹, T. Alt³⁵, V. Altini²⁷, S. Altinpinar¹⁴, I. Altsybeev¹¹⁶, C. Andrei⁷⁰, A. Andronic⁸⁵, V. Anguelov⁸², J. Anielski⁵⁴, C. Anson¹⁵, T. Antičić⁸⁶, F. Antinori⁹³, P. Antonioli⁹⁷, L. Aphecetche¹⁰², H. Appelshäuser⁵², N. Arbor⁶⁴, S. Arcelli²¹, A. Arend⁵², N. Armesto¹², R. Arnaldi⁹⁴, T. Aronsson¹¹⁹, I.C. Arsene⁸⁵, M. Arslanok⁵², A. Asryan¹¹⁶, A. Augustinus²⁹, R. Averbeck⁸⁵, T.C. Awes⁷⁴, J. Åystö³⁷, M.D. Azmi¹³, M. Bach³⁵, A. Badalá⁹⁹, Y.W. Baek^{63,36}, R. Bailhache⁵², R. Bala⁹⁴, R. Baldini Ferrolí⁹, A. Baldisseri¹¹, A. Baldit⁶³, F. Baltasar Dos Santos Pedrosa²⁹, J. Bán⁴⁷, R.C. Baral⁴⁸, R. Barbera²³, F. Barile²⁷, G.G. Barnaföldi⁶⁰, L.S. Barnby⁹⁰, V. Barret⁶³, J. Bartke¹⁰⁴, M. Basile²¹, N. Bastid⁶³, S. Basu¹¹⁵, B. Bathen⁵⁴, G. Batigne¹⁰², B. Batyunya⁵⁹, C. Baumann⁵², I.G. Bearden⁷¹, H. Beck⁵², I. Belikov⁵⁸, F. Bellini²¹, R. Bellwied¹¹⁰, E. Belmont-Moreno⁵⁶, G. Bencedi⁶⁰, S. Beole²⁵, I. Berceanu⁷⁰, A. Bercuci⁷⁰, Y. Berdnikov⁷⁵, D. Berenyi⁶⁰, D. Berzano⁹⁴, L. Betev²⁹, A. Bhasin⁸⁰, A.K. Bhati⁷⁷, J. Bhom¹¹³, N. Bianchi⁶⁵, L. Bianchi²⁵, C. Bianchin¹⁹, J. Bielčik³³, J. Bielčíková⁷³, A. Bilandžić^{72,71}, S. Bjelogrić⁴⁵, F. Blanco⁷, F. Blanco¹¹⁰, D. Blau⁸⁸, C. Blume⁵², M. Boccioni²⁹, N. Bock¹⁵, A. Bogdanov⁶⁹, H. Bøggild⁷¹, M. Bogolyubsky⁴³, L. Boldizsár⁶⁰, M. Bombara³⁴, J. Book⁵², H. Borel¹¹, A. Borissov¹¹⁸, S. Bose⁸⁹, F. Bossú²⁵, M. Botje⁷², S. Böttger⁵¹, B. Boyer⁴², E. Braidot⁶⁷, P. Braun-Munzinger⁸⁵, M. Bregant¹⁰², T. Breitner⁵¹, T.A. Browning⁸³, M. Broz³², R. Brun²⁹, E. Bruna^{25,94}, G.E. Bruno²⁷, D. Budnikov⁸⁷, H. Buesching⁵², S. Bufalino^{25,94}, K. Bugaiev², O. Busch⁸², Z. Buthelezi⁷⁹, D. Caballero Orduna¹¹⁹, D. Caffarri¹⁹, X. Cai³⁹, H. Caines¹¹⁹, E. Calvo Villar⁹¹, P. Camerini²⁰, V. Canoa Roman^{8,1}, G. Cara Romeo⁹⁷, W. Carena²⁹, F. Carena²⁹, N. Carlin Filho¹⁰⁷, F. Carminati²⁹, C.A. Carrillo Montoya²⁹, A. Casanova Díaz⁶⁵, J. Castillo Castellanos¹¹, J.F. Castillo Hernandez⁸⁵, E.A.R. Casula¹⁸, V. Catanescu⁷⁰, C. Cavicchioli²⁹, C. Ceballos Sanchez⁶, J. Cepila³³, P. Cerello⁹⁴, B. Chang^{37,122}, S. Chapeland²⁹, J.L. Charvet¹¹, S. Chattopadhyay⁸⁹, S. Chattopadhyay¹¹⁵, I. Chawla⁷⁷, M. Cherneny⁷⁶, C. Cheshkov^{29,109}, B. Cheynis¹⁰⁹, V. Chibante Barroso²⁹, D.D. Chinellato¹⁰⁸, P. Chochula²⁹, M. Chojnacki⁴⁵, S. Choudhury¹¹⁵, P. Christakoglou^{72,45}, C.H. Christensen⁷¹, P. Christiansen²⁸, T. Chujo¹¹³, S.U. Chung⁸⁴, C. Cicalo⁹⁶, L. Cifarelli^{21,29}, F. Cindolo⁹⁷, J. Cleymans⁷⁹, F. Coccetti⁹, F. Colamaria²⁷, D. Colella²⁷, G. Conesa Balbastre⁶⁴, Z. Conesa del Valle²⁹, P. Constantin⁸², G. Contin²⁰, J.G. Contreras⁸, T.M. Cormier¹¹⁸, Y. Corrales Morales²⁵, P. Cortese²⁶, I. Cortés Maldonado¹, M.R. Cosentino^{67,108}, F. Costa²⁹, M.E. Cotallo⁷, E. Crescio⁸, P. Crochet⁶³, E. Cruz Alaniz⁵⁶, E. Cuautle⁵⁵, L. Cunqueiro⁶⁵, A. Dainese^{19,93}, H.H. Dalsgaard⁷¹, A. Danu⁵⁰, K. Das⁸⁹, I. Das^{89,42}, D. Das⁸⁹, A. Dash¹⁰⁸, S. Dash⁴⁰, S. De¹¹⁵, G.O.V. de Barros¹⁰⁷, A. De Caro^{24,9}, G. de Cataldo⁹⁸, J. de Cuijland³⁵, A. De Falco¹⁸, D. De Gruttola²⁴, H. Delagrangé¹⁰², E. Del Castillo Sanchez²⁹, A. Deloff¹⁰⁰, V. Demanov⁸⁷, N. De Marco⁹⁴, E. Dénes⁶⁰, S. De Pasquale²⁴, A. Deppman¹⁰⁷, G. D'Erasmus²⁷, R. de Rooij⁴⁵, M.A. Diaz Corchero⁷, D. Di Bari²⁷,

T. Dietel⁵⁴, C. Di Giglio²⁷, S. Di Liberto⁹⁵, A. Di Mauro²⁹, P. Di Nezza⁶⁵, R. Divià²⁹, Ø. Djuvsland¹⁴, A. Dobrin^{118,28}, T. Dobrowolski¹⁰⁰, I. Domínguez⁵⁵, B. Dönigus⁸⁵, O. Dordic¹⁷, O. Driga¹⁰², A.K. Dubey¹¹⁵, L. Ducroux¹⁰⁹, P. Dupieux⁶³, A.K. Dutta Majumdar⁸⁹, M.R. Dutta Majumdar¹¹⁵, D. Elia⁹⁸, D. Emschermann⁵⁴, H. Engel⁵¹, H.A. Erdal³¹, B. Espagnon⁴², M. Estienne¹⁰², S. Esumi¹¹³, D. Evans⁹⁰, G. Eyyubova¹⁷, D. Fabris^{19,93}, J. Faivre⁶⁴, D. Falchieri²¹, A. Fantoni⁶⁵, M. Fasel⁸⁵, R. Fearick⁷⁹, A. Fedunov⁵⁹, D. Fehlker¹⁴, L. Feldkamp⁵⁴, D. Felea⁵⁰, B. Fenton-Olsen⁶⁷, G. Feofilov¹¹⁶, A. Fernández Téllez¹, A. Ferretti²⁵, R. Ferretti²⁶, J. Figiel¹⁰⁴, M.A.S. Figueredo¹⁰⁷, S. Filchagin⁸⁷, D. Finogeev⁴⁴, F.M. Fionda²⁷, E.M. Fiore²⁷, M. Floris²⁹, S. Foertsch⁷⁹, P. Foka⁸⁵, S. Fokin⁸⁸, E. Fragiaco⁹², M. Fragkiadakis⁷⁸, U. Frankenfeld⁸⁵, U. Fuchs²⁹, C. Furget⁶⁴, M. Fusco Girard²⁴, J.J. Gaardhøje⁷¹, M. Gagliardi²⁵, A. Gago⁹¹, M. Gallio²⁵, D.R. Gangadharan¹⁵, P. Ganoti⁷⁴, C. Garabatos⁸⁵, E. Garcia-Solis¹⁰, I. Garishvili⁶⁸, J. Gerhard³⁵, M. Germain¹⁰², C. Geuna¹¹, M. Gheata²⁹, A. Gheata²⁹, B. Ghidini²⁷, P. Ghosh¹¹⁵, P. Gianotti⁶⁵, M.R. Girard¹¹⁷, P. Giubellino²⁹, E. Gladysz-Dziadus¹⁰⁴, P. Glässel⁸², R. Gomez¹⁰⁶, E.G. Ferreira¹², L.H. González-Trueba⁵⁶, P. González-Zamora⁷, S. Gorbunov³⁵, A. Goswami⁸¹, S. Gotovac¹⁰³, V. Grabski⁵⁶, L.K. Graczykowski¹¹⁷, R. Grajcarek⁸², A. Grelli⁴⁵, C. Grigoras²⁹, A. Grigoras²⁹, V. Grigoriev⁶⁹, S. Grigoryan⁵⁹, A. Grigoryan¹²⁰, B. Grinyov², N. Grion⁹², P. Gros²⁸, J.F. Grosse-Oetringhaus²⁹, J.-Y. Grossiord¹⁰⁹, R. Grosso²⁹, F. Guber⁴⁴, R. Guernane⁶⁴, C. Guerra Gutierrez⁹¹, B. Guerzoni²¹, M. Guilbaud¹⁰⁹, K. Gulbrandsen⁷¹, T. Gunji¹¹², R. Gupta⁸⁰, A. Gupta⁸⁰, H. Gutbrod⁸⁵, Ø. Haaland¹⁴, C. Hadjidakis⁴², M. Haiduc⁵⁰, H. Hamagaki¹¹², G. Hamar⁶⁰, B.H. Han¹⁶, L.D. Hanratty⁹⁰, A. Hansen⁷¹, Z. Harmanova³⁴, J.W. Harris¹¹⁹, M. Hartig⁵², D. Hasegan⁵⁰, D. Hatzifotiadou⁹⁷, A. Hayrapetyan^{29,120}, S.T. Heckel⁵², M. Heide⁵⁴, H. Helstrup³¹, A. Herghelegiu⁷⁰, G. Herrera Corral⁸, N. Herrmann⁸², K.F. Hetland³¹, B. Hicks¹¹⁹, P.T. Hille¹¹⁹, B. Hippolyte⁵⁸, T. Horaguchi¹¹³, Y. Hori¹¹², P. Hristov²⁹, I. Hřivnáčová⁴², M. Huang¹⁴, T.J. Humanic¹⁵, D.S. Hwang¹⁶, R. Ichou⁶³, R. Ilkaev⁸⁷, I. Ilkiv¹⁰⁰, M. Inaba¹¹³, E. Incani¹⁸, P.G. Innocenti²⁹, G.M. Innocenti²⁵, M. Ippolitov⁸⁸, M. Irfan¹³, C. Ivan⁸⁵, V. Ivanov⁷⁵, A. Ivanov¹¹⁶, M. Ivanov⁸⁵, O. Ivanytskyi², A. Jachořkowski²⁹, P. M. Jacobs⁶⁷, L. Jancurová⁵⁹, H.J. Jang⁶², S. Jangal⁵⁸, R. Janik³², M.A. Janik¹¹⁷, P.H.S.Y. Jayarathna¹¹⁰, S. Jena⁴⁰, D.M. Jha¹¹⁸, R.T. Jimenez Bustamante⁵⁵, L. Jirden²⁹, P.G. Jones⁹⁰, H. Jung³⁶, A. Jusko⁹⁰, A.B. Kaidalov⁴⁶, V. Kakoyan¹²⁰, S. Kalcher³⁵, P. Kaliňák⁴⁷, M. Kalisky⁵⁴, T. Kalliokoski³⁷, A. Kalweit⁵³, K. Kanaki¹⁴, J.H. Kang¹²², V. Kaplin⁶⁹, A. Karasu Uysal^{29,121}, O. Karavichev⁴⁴, T. Karavicheva⁴⁴, E. Karpechev⁴⁴, A. Kazantsev⁸⁸, U. Kebschull⁵¹, R. Keidel¹²³, M.M. Khan¹³, S.A. Khan¹¹⁵, A. Khanzadeev⁷⁵, Y. Kharlov⁴³, B. Kileng³¹, J.S. Kim³⁶, D.W. Kim³⁶, S.H. Kim³⁶, J.H. Kim¹⁶, M. Kim¹²², D.J. Kim³⁷, B. Kim¹²², T. Kim¹²², S. Kim¹⁶, S. Kirsch³⁵, I. Kisel³⁵, S. Kiselev⁴⁶, A. Kisiel^{29,117}, J.L. Klay⁴, J. Klein⁸², C. Klein-Bösing⁵⁴, M. Kliemant⁵², A. Kluge²⁹, M.L. Knichel⁸⁵, A.G. Knospe¹⁰⁵, K. Koch⁸², M.K. Köhler⁸⁵, A. Kolojvari¹¹⁶, V. Kondratiev¹¹⁶, N. Kondratyeva⁶⁹, A. Konevskikh⁴⁴, A. Korneev⁸⁷, R. Kour⁹⁰, M. Kowalski¹⁰⁴, S. Kox⁶⁴, G. Koyithatta Meethaleveedu⁴⁰, J. Kral³⁷, I. Králík⁴⁷, F. Kramer⁵², I. Kraus⁸⁵, T. Krawutschke^{82,30}, M. Krelna³³, M. Kretz³⁵, M. Krivda^{90,47}, F. Krizek³⁷, M. Krus³³, E. Kryshen⁷⁵, M. Krzewicki^{72,85}, Y. Kucheriaev⁸⁸, C. Kuhn⁵⁸, P.G. Kuijter⁷², P. Kurashvili¹⁰⁰, A. Kurepin⁴⁴, A.B. Kurepin⁴⁴, A. Kuryakin⁸⁷, V. Kuschpil⁷³, S. Kuschpil⁷³, H. Kvaerno¹⁷, M.J. Kweon⁸², Y. Kwon¹²², P. Ladrón de Guevara⁵⁵, I. Lakomov^{42,116}, R. Langoy¹⁴, S.L. La Pointe⁴⁵, C. Lara⁵¹, A. Lardeux¹⁰², P. La Rocca²³, C. Lazzeroni⁹⁰, R. Lea²⁰, Y. Le Bornec⁴², M. Lechman²⁹, S.C. Lee³⁶, K.S. Lee³⁶, F. Lefèvre¹⁰², J. Lehnert⁵², L. Leistam²⁹, M. Lenhardt¹⁰², V. Lenti⁹⁸, H. León⁵⁶, I. León Monzón¹⁰⁶, H. León Vargas⁵², P. Lévi⁶⁰, J. Lien¹⁴, R. Lietava⁹⁰, S. Lindal¹⁷, V. Lindenstruth³⁵, C. Lippmann^{85,29}, M.A. Lisa¹⁵, L. Liu¹⁴, P.I. Loenne¹⁴, V.R. Loggins¹¹⁸, V. Loginov⁶⁹, S. Lohn²⁹, D. Lohner⁸², C. Loizides⁶⁷, K.K. Loo³⁷, X. Lopez⁶³, E. López Torres⁶, G. Løvhøiden¹⁷, X.-G. Lu⁸², P. Luettig⁵², M. Lunardon¹⁹, J. Luo³⁹, G. Luparello⁴⁵, L. Luquin¹⁰², C. Luzzi²⁹, R. Ma¹¹⁹, K. Ma³⁹, D.M. Madagodahettige-Don¹¹⁰, A. Maevskaya⁴⁴, M. Mager^{53,29}, D.P. Mahapatra⁴⁸, A. Maire⁵⁸, M. Malaev⁷⁵, I. Maldonado Cervantes⁵⁵, L. Malinina^{59,1}, D. Mal'Kevich⁴⁶, P. Malzacher⁸⁵, A. Mamonov⁸⁷, L. Manceau⁹⁴, L. Mangotra⁸⁰, V. Manko⁸⁸, F. Manso⁶³, V. Manzari⁹⁸, Y. Mao^{64,39}, M. Marchionese^{63,25}, J. Mareš⁴⁹, G.V. Margagliotti^{20,92}, A. Margotti⁹⁷, A. Marín⁸⁵, C.A. Marin Tobon²⁹, C. Markert¹⁰⁵, I. Martashvili¹¹¹, P. Martinengo²⁹, M.I. Martínez¹, A. Martínez Davalos⁵⁶, G. Martínez García¹⁰², Y. Martynov², A. Mas¹⁰², S. Masciocchi⁸⁵, M. Masera²⁵, A. Masoni⁹⁶, L. Massacrier^{109,102}, M. Mastromarco⁹⁸, A. Mastroserio^{27,29}, Z.L. Matthews⁹⁰, A. Matyja^{104,102}, D. Mayani⁵⁵, C. Mayer¹⁰⁴, J. Mazer¹¹¹, M.A. Mazzoni⁹⁵, F. Meddi²², A. Menchaca-Rocha⁵⁶, J. Mercado Pérez⁸², M. Meres³², Y. Miake¹¹³, L. Milano²⁵, J. Milosevic^{17,111},

A. Mischke⁴⁵, A.N. Mishra⁸¹, D. Miśkowiec^{85, 29}, C. Mitu⁵⁰, J. Mlynarz¹¹⁸, A.K. Mohanty²⁹, B. Mohanty¹¹⁵, L. Molnar²⁹, L. Montaño Zetina⁸, M. Monteno⁹⁴, E. Montes⁷, T. Moon¹²², M. Morando¹⁹, D.A. Moreira De Godoy¹⁰⁷, S. Moretto¹⁹, A. Morsch²⁹, V. Muccifora⁶⁵, E. Mudnic¹⁰³, S. Muhuri¹¹⁵, M. Mukherjee¹¹⁵, H. Müller²⁹, M.G. Munhoz¹⁰⁷, L. Musa²⁹, A. Musso⁹⁴, B.K. Nandi⁴⁰, R. Nania⁹⁷, E. Nappi⁹⁸, C. Natrass¹¹¹, N.P. Naumov⁸⁷, S. Navin⁹⁰, T.K. Nayak¹¹⁵, S. Nazarenko⁸⁷, G. Nazarov⁸⁷, A. Nedosekin⁴⁶, M. Nicassio²⁷, B.S. Nielsen⁷¹, T. Niida¹¹³, S. Nikolaev⁸⁸, V. Nikolic⁸⁶, V. Nikulin⁷⁵, S. Nikulin⁸⁸, B.S. Nilsen⁷⁶, M.S. Nilsson¹⁷, F. Noferini^{97, 9}, P. Nomokonov⁵⁹, G. Nooren⁴⁵, N. Novitzky³⁷, A. Nyanin⁸⁸, A. Nyatha⁴⁰, C. Nygaard⁷¹, J. Nystrand¹⁴, A. Ochirov¹¹⁶, H. Oeschler^{53, 29}, S. Oh¹¹⁹, S.K. Oh³⁶, J. Oleniacz¹¹⁷, C. Oppedisano⁹⁴, A. Ortiz Velasquez^{28, 55}, G. Ortona²⁵, A. Oskarsson²⁸, P. Ostrowski¹¹⁷, J. Otwinowski⁸⁵, K. Oyama⁸², K. Ozawa¹¹², Y. Pachmayer⁸², M. Pachr³³, F. Padilla²⁵, P. Pagano²⁴, G. Paic⁵⁵, F. Painke³⁵, C. Pajares¹², S.K. Pal¹¹⁵, S. Pal¹¹, A. Palaha⁹⁰, A. Palmeri⁹⁹, V. Papikyan¹²⁰, G.S. Pappalardo⁹⁹, W.J. Park⁸⁵, A. Passfeld⁵⁴, B. Pastirčák⁴⁷, D.I. Patalakha⁴³, V. Paticchio⁹⁸, A. Pavlinov¹¹⁸, T. Pawlak¹¹⁷, T. Peitzmann⁴⁵, H. Pereira Da Costa¹¹, E. Pereira De Oliveira Filho¹⁰⁷, D. Peresunko⁸⁸, C.E. Pérez Lara⁷², E. Perez Lezama⁵⁵, D. Perini²⁹, D. Perrino²⁷, W. Peryt¹¹⁷, A. Pesci⁹⁷, V. Peskov^{29, 55}, Y. Pestov³, V. Petráček³³, M. Petran³³, M. Petris⁷⁰, P. Petrov⁹⁰, M. Petrovici⁷⁰, C. Petta²³, S. Piano⁹², A. Piccotti⁹⁴, M. Pikna³², P. Pillot¹⁰², O. Pinazza²⁹, L. Pinsky¹¹⁰, N. Pitz⁵², D.B. Piyarathna¹¹⁰, M. Płoskoń⁶⁷, J. Pluta¹¹⁷, T. Pocheptsov⁵⁹, S. Pochybova⁶⁰, P.L.M. Podesta-Lerma¹⁰⁶, M.G. Poghosyan^{29, 25}, K. Polák⁴⁹, B. Polichtchouk⁴³, A. Pop⁷⁰, S. Porteboeuf-Houssais⁶³, V. Pospíšil³³, B. Potukuchi⁸⁰, S.K. Prasad¹¹⁸, R. Preghenella^{97, 9}, F. Prino⁹⁴, C.A. Pruneau¹¹⁸, I. Pshenichnov⁴⁴, S. Puchagin⁸⁷, G. Puddu¹⁸, J. Pujol Teixido⁵¹, A. Pulvirenti^{23, 29}, V. Punin⁸⁷, M. Putiš³⁴, J. Putschke^{118, 119}, E. Quercigh²⁹, H. Qvigstad¹⁷, A. Rachevski⁹², A. Rademakers²⁹, S. Radomski⁸², T.S. Rähä³⁷, J. Rak³⁷, A. Rakotozafindrabe¹¹, L. Ramello²⁶, A. Ramírez Reyes⁸, R. Raniwala⁸¹, S. Raniwala⁸¹, S.S. Räsänen³⁷, B.T. Rascanu⁵², D. Rathee⁷⁷, K.F. Read¹¹¹, J.S. Real⁶⁴, K. Redlich^{100, 57}, P. Reichelt⁵², M. Reicher⁴⁵, R. Renfordt⁵², A.R. Reolon⁶⁵, A. Reshetin⁴⁴, F. Rettig³⁵, J.-P. Revol²⁹, K. Reygiers⁸², L. Riccati⁹⁴, R.A. Ricci⁶⁶, T. Richert²⁸, M. Richter¹⁷, P. Riedler²⁹, W. Riegler²⁹, F. Riggi^{23, 99}, B. Rodrigues Fernandes Rabacal²⁹, M. Rodríguez Cahuantzi¹, A. Rodríguez Manso⁷², K. Røed¹⁴, D. Rohr³⁵, D. Röhrich¹⁴, R. Romita⁸⁵, F. Ronchetti⁶⁵, P. Rosnet⁶³, S. Rossegger²⁹, A. Rossi¹⁹, F. Roukoutakis⁷⁸, P. Roy⁸⁹, C. Roy⁵⁸, A.J. Rubio Montero⁷, R. Rui²⁰, E. Ryabinkin⁸⁸, A. Rybicki¹⁰⁴, S. Sadovsky⁴³, K. Šafařík²⁹, R. Sahoo⁴¹, P.K. Sahu⁴⁸, J. Saini¹¹⁵, H. Sakaguchi³⁸, S. Sakai⁶⁷, D. Sakata¹¹³, C.A. Salgado¹², J. Salzwedel¹⁵, S. Sambyal⁸⁰, V. Samsonov⁷⁵, X. Sanchez Castro^{55, 58}, L. Šándor⁴⁷, A. Sandoval⁵⁶, S. Sano¹¹², M. Sano¹¹³, R. Santo⁵⁴, R. Santoro^{98, 29}, J. Sarkamo³⁷, E. Scapparone⁹⁷, F. Scarlassara¹⁹, R.P. Scharenberg⁸³, C. Schiaua⁷⁰, R. Schicker⁸², C. Schmidt⁸⁵, H.R. Schmidt^{85, 114}, S. Schreiner²⁹, S. Schuchmann⁵², J. Schukraft²⁹, Y. Schutz^{29, 102}, K. Schwarz⁸⁵, K. Schweda^{85, 82}, G. Scioli²¹, E. Scomparin⁹⁴, R. Scott¹¹¹, P.A. Scott⁹⁰, G. Segato¹⁹, I. Selyuzhenkov⁸⁵, S. Senyukov^{26, 58}, J. Seo⁸⁴, S. Serici¹⁸, E. Serradilla^{7, 56}, A. Sevcenco⁵⁰, I. Sgura⁹⁸, A. Shabetai¹⁰², G. Shabratova⁵⁹, R. Shahoyan²⁹, N. Sharma⁷⁷, S. Sharma⁸⁰, K. Shigaki³⁸, M. Shimomura¹¹³, K. Shtejer⁶, Y. Sibiriak⁸⁸, M. Siciliano²⁵, E. Sicking²⁹, S. Siddhanta⁹⁶, T. Siemiarczuk¹⁰⁰, D. Silvermyr⁷⁴, c. Silvestre⁶⁴, G. Simonetti^{27, 29}, R. Singaraju¹¹⁵, R. Singh⁸⁰, S. Singha¹¹⁵, B.C. Sinha¹¹⁵, T. Sinha⁸⁹, B. Sitar³², M. Sitta²⁶, T.B. Skaali¹⁷, K. Skjerdal¹⁴, R. Smakal³³, N. Smirnov¹¹⁹, R.J.M. Snellings⁴⁵, C. Sjøgaard⁷¹, R. Soltz⁶⁸, H. Son¹⁶, M. Song¹²², J. Song⁸⁴, C. Soos²⁹, F. Soramel¹⁹, I. Sputowska¹⁰⁴, M. Spyropoulou-Stassinaki⁷⁸, B.K. Srivastava⁸³, J. Stachel⁸², I. Stan⁵⁰, I. Stan⁵⁰, G. Stefanek¹⁰⁰, T. Steinbeck³⁵, M. Steinpreis¹⁵, E. Stenlund²⁸, G. Steyn⁷⁹, J.H. Stiller⁸², D. Stocco¹⁰², M. Stolpovskiy⁴³, K. Strabykin⁸⁷, P. Strmen³², A.A.P. Suaide¹⁰⁷, M.A. Subieta Vásquez²⁵, T. Sugitate³⁸, C. Suire⁴², M. Sukhorukov⁸⁷, R. Sultanov⁴⁶, M. Šumbera⁷³, T. Susa⁸⁶, A. Szanto de Toledo¹⁰⁷, I. Szarka³², A. Szostak¹⁴, C. Tagridis⁷⁸, J. Takahashi¹⁰⁸, J.D. Tapia Takaki⁴², A. Tauro²⁹, G. Tejeda Muñoz¹, A. Telesca²⁹, C. Terrevoli²⁷, J. Thäder⁸⁵, D. Thomas⁴⁵, R. Tieulent¹⁰⁹, A.R. Timmins¹¹⁰, D. Tlusty³³, A. Toia^{35, 29}, H. Torii^{38, 112}, L. Toscano⁹⁴, D. Truesdale¹⁵, W.H. Trzaska³⁷, T. Tsuji¹¹², A. Tumkin⁸⁷, R. Turrisi⁹³, T.S. Tveter¹⁷, J. Ulery⁵², K. Ullaland¹⁴, J. Ulrich^{61, 51}, A. Uras¹⁰⁹, J. Urbán³⁴, G.M. Urciuoli⁹⁵, G.L. Usai¹⁸, M. Vajzer^{33, 73}, M. Vala^{59, 47}, L. Valencia Palomo⁴², S. Vallero⁸², N. van der Kolk⁷², P. Vande Vyve²⁹, M. van Leeuwen⁴⁵, L. Vannucci⁶⁶, A. Vargas¹, R. Varma⁴⁰, M. Vasileiou⁷⁸, A. Vasiliev⁸⁸, V. Vechernin¹¹⁶, M. Veldhoen⁴⁵, M. Venaruzzo²⁰, E. Vercellin²⁵, S. Vergara¹, R. Vernet⁵, M. Verweij⁴⁵, L. Vickovic¹⁰³, G. Viesti¹⁹, O. Vikhlyantsev⁸⁷, Z. Vilakazi⁷⁹, O. Villalobos Baillie⁹⁰, A. Vinogradov⁸⁸, L. Vinogradov¹¹⁶, Y. Vinogradov⁸⁷, T. Virgili²⁴, Y.P. Viyogi¹¹⁵, A. Vodopyanov⁵⁹, S. Voloshin¹¹⁸, K. Voloshin⁴⁶, G. Volpe^{27, 29},

B. von Haller²⁹, D. Vranic⁸⁵, G. Øvrebek¹⁴, J. Vrláková³⁴, B. Vulpescu⁶³, A. Vyushin⁸⁷, B. Wagner¹⁴, V. Wagner³³, R. Wan^{58,39}, Y. Wang⁸², D. Wang³⁹, Y. Wang³⁹, M. Wang³⁹, K. Watanabe¹¹³, J.P. Wessels^{29,54}, U. Westerhoff⁵⁴, J. Wiechula¹¹⁴, J. Wikne¹⁷, M. Wilde⁵⁴, G. Wilk¹⁰⁰, A. Wilk⁵⁴, M.C.S. Williams⁹⁷, B. Windelband⁸², L. Xaplanteris Karampatos¹⁰⁵, C.G. Yaldo¹¹⁸, H. Yang¹¹, S. Yang¹⁴, S. Yasnopolskiy⁸⁸, J. Yi⁸⁴, Z. Yin³⁹, I.-K. Yoo⁸⁴, J. Yoon¹²², W. Yu⁵², X. Yuan³⁹, I. Yushmanov⁸⁸, C. Zach³³, C. Zampolli⁹⁷, S. Zaporozhets⁵⁹, A. Zarochentsev¹¹⁶, P. Závada⁴⁹, N. Zaviyalov⁸⁷, H. Zbroszczyk¹¹⁷, P. Zelnicsek⁵¹, I.S. Zgura⁵⁰, M. Zhalov⁷⁵, H. Zhang³⁹, X. Zhang^{63,39}, D. Zhou³⁹, F. Zhou³⁹, Y. Zhou⁴⁵, X. Zhu³⁹, J. Zhu³⁹, J. Zhu³⁹, A. Zichichi^{21,9}, A. Zimmermann⁸², G. Zinovjev², Y. Zoccarato¹⁰⁹, M. Zynovyev²

Affiliation notes

ⁱ Also at: M.V.Lomonosov Moscow State University, D.V.Skobeltzyn Institute of Nuclear Physics, Moscow, Russia

ⁱⁱ Also at: "Vinča" Institute of Nuclear Sciences, Belgrade, Serbia

Collaboration Institutes

- ¹ Benemérita Universidad Autónoma de Puebla, Puebla, Mexico
- ² Bogolyubov Institute for Theoretical Physics, Kiev, Ukraine
- ³ Budker Institute for Nuclear Physics, Novosibirsk, Russia
- ⁴ California Polytechnic State University, San Luis Obispo, California, United States
- ⁵ Centre de Calcul de l'IN2P3, Villeurbanne, France
- ⁶ Centro de Aplicaciones Tecnológicas y Desarrollo Nuclear (CEADEN), Havana, Cuba
- ⁷ Centro de Investigaciones Energéticas Medioambientales y Tecnológicas (CIEMAT), Madrid, Spain
- ⁸ Centro de Investigación y de Estudios Avanzados (CINVESTAV), Mexico City and Mérida, Mexico
- ⁹ Centro Fermi – Centro Studi e Ricerche e Museo Storico della Fisica "Enrico Fermi", Rome, Italy
- ¹⁰ Chicago State University, Chicago, United States
- ¹¹ Commissariat à l'Energie Atomique, IRFU, Saclay, France
- ¹² Departamento de Física de Partículas and IGFAE, Universidad de Santiago de Compostela, Santiago de Compostela, Spain
- ¹³ Department of Physics Aligarh Muslim University, Aligarh, India
- ¹⁴ Department of Physics and Technology, University of Bergen, Bergen, Norway
- ¹⁵ Department of Physics, Ohio State University, Columbus, Ohio, United States
- ¹⁶ Department of Physics, Sejong University, Seoul, South Korea
- ¹⁷ Department of Physics, University of Oslo, Oslo, Norway
- ¹⁸ Dipartimento di Fisica dell'Università and Sezione INFN, Cagliari, Italy
- ¹⁹ Dipartimento di Fisica dell'Università and Sezione INFN, Padova, Italy
- ²⁰ Dipartimento di Fisica dell'Università and Sezione INFN, Trieste, Italy
- ²¹ Dipartimento di Fisica dell'Università and Sezione INFN, Bologna, Italy
- ²² Dipartimento di Fisica dell'Università 'La Sapienza' and Sezione INFN, Rome, Italy
- ²³ Dipartimento di Fisica e Astronomia dell'Università and Sezione INFN, Catania, Italy
- ²⁴ Dipartimento di Fisica 'E.R. Caianiello' dell'Università and Gruppo Collegato INFN, Salerno, Italy
- ²⁵ Dipartimento di Fisica Sperimentale dell'Università and Sezione INFN, Turin, Italy
- ²⁶ Dipartimento di Scienze e Tecnologie Avanzate dell'Università del Piemonte Orientale and Gruppo Collegato INFN, Alessandria, Italy
- ²⁷ Dipartimento Interateneo di Fisica 'M. Merlin' and Sezione INFN, Bari, Italy
- ²⁸ Division of Experimental High Energy Physics, University of Lund, Lund, Sweden
- ²⁹ European Organization for Nuclear Research (CERN), Geneva, Switzerland
- ³⁰ Fachhochschule Köln, Köln, Germany
- ³¹ Faculty of Engineering, Bergen University College, Bergen, Norway
- ³² Faculty of Mathematics, Physics and Informatics, Comenius University, Bratislava, Slovakia

- 33 Faculty of Nuclear Sciences and Physical Engineering, Czech Technical University in Prague, Prague, Czech Republic
- 34 Faculty of Science, P.J. Šafárik University, Košice, Slovakia
- 35 Frankfurt Institute for Advanced Studies, Johann Wolfgang Goethe-Universität Frankfurt, Frankfurt, Germany
- 36 Gangneung-Wonju National University, Gangneung, South Korea
- 37 Helsinki Institute of Physics (HIP) and University of Jyväskylä, Jyväskylä, Finland
- 38 Hiroshima University, Hiroshima, Japan
- 39 Hua-Zhong Normal University, Wuhan, China
- 40 Indian Institute of Technology, Mumbai, India
- 41 Indian Institute of Technology Indore (IIT), Indore, India
- 42 Institut de Physique Nucléaire d'Orsay (IPNO), Université Paris-Sud, CNRS-IN2P3, Orsay, France
- 43 Institute for High Energy Physics, Protvino, Russia
- 44 Institute for Nuclear Research, Academy of Sciences, Moscow, Russia
- 45 Nikhef, National Institute for Subatomic Physics and Institute for Subatomic Physics of Utrecht University, Utrecht, Netherlands
- 46 Institute for Theoretical and Experimental Physics, Moscow, Russia
- 47 Institute of Experimental Physics, Slovak Academy of Sciences, Košice, Slovakia
- 48 Institute of Physics, Bhubaneswar, India
- 49 Institute of Physics, Academy of Sciences of the Czech Republic, Prague, Czech Republic
- 50 Institute of Space Sciences (ISS), Bucharest, Romania
- 51 Institut für Informatik, Johann Wolfgang Goethe-Universität Frankfurt, Frankfurt, Germany
- 52 Institut für Kernphysik, Johann Wolfgang Goethe-Universität Frankfurt, Frankfurt, Germany
- 53 Institut für Kernphysik, Technische Universität Darmstadt, Darmstadt, Germany
- 54 Institut für Kernphysik, Westfälische Wilhelms-Universität Münster, Münster, Germany
- 55 Instituto de Ciencias Nucleares, Universidad Nacional Autónoma de México, Mexico City, Mexico
- 56 Instituto de Física, Universidad Nacional Autónoma de México, Mexico City, Mexico
- 57 Institut of Theoretical Physics, University of Wrocław
- 58 Institut Pluridisciplinaire Hubert Curien (IPHC), Université de Strasbourg, CNRS-IN2P3, Strasbourg, France
- 59 Joint Institute for Nuclear Research (JINR), Dubna, Russia
- 60 KFKI Research Institute for Particle and Nuclear Physics, Hungarian Academy of Sciences, Budapest, Hungary
- 61 Kirchhoff-Institut für Physik, Ruprecht-Karls-Universität Heidelberg, Heidelberg, Germany
- 62 Korea Institute of Science and Technology Information, Daejeon, South Korea
- 63 Laboratoire de Physique Corpusculaire (LPC), Clermont Université, Université Blaise Pascal, CNRS-IN2P3, Clermont-Ferrand, France
- 64 Laboratoire de Physique Subatomique et de Cosmologie (LPSC), Université Joseph Fourier, CNRS-IN2P3, Institut Polytechnique de Grenoble, Grenoble, France
- 65 Laboratori Nazionali di Frascati, INFN, Frascati, Italy
- 66 Laboratori Nazionali di Legnaro, INFN, Legnaro, Italy
- 67 Lawrence Berkeley National Laboratory, Berkeley, California, United States
- 68 Lawrence Livermore National Laboratory, Livermore, California, United States
- 69 Moscow Engineering Physics Institute, Moscow, Russia
- 70 National Institute for Physics and Nuclear Engineering, Bucharest, Romania
- 71 Niels Bohr Institute, University of Copenhagen, Copenhagen, Denmark
- 72 Nikhef, National Institute for Subatomic Physics, Amsterdam, Netherlands
- 73 Nuclear Physics Institute, Academy of Sciences of the Czech Republic, Řež u Prahy, Czech Republic
- 74 Oak Ridge National Laboratory, Oak Ridge, Tennessee, United States
- 75 Petersburg Nuclear Physics Institute, Gatchina, Russia
- 76 Physics Department, Creighton University, Omaha, Nebraska, United States
- 77 Physics Department, Panjab University, Chandigarh, India

- 78 Physics Department, University of Athens, Athens, Greece
- 79 Physics Department, University of Cape Town, iThemba LABS, Cape Town, South Africa
- 80 Physics Department, University of Jammu, Jammu, India
- 81 Physics Department, University of Rajasthan, Jaipur, India
- 82 Physikalisches Institut, Ruprecht-Karls-Universität Heidelberg, Heidelberg, Germany
- 83 Purdue University, West Lafayette, Indiana, United States
- 84 Pusan National University, Pusan, South Korea
- 85 Research Division and ExtreMe Matter Institute EMMI, GSI Helmholtzzentrum für Schwerionenforschung, Darmstadt, Germany
- 86 Rudjer Bošković Institute, Zagreb, Croatia
- 87 Russian Federal Nuclear Center (VNIIEF), Sarov, Russia
- 88 Russian Research Centre Kurchatov Institute, Moscow, Russia
- 89 Saha Institute of Nuclear Physics, Kolkata, India
- 90 School of Physics and Astronomy, University of Birmingham, Birmingham, United Kingdom
- 91 Sección Física, Departamento de Ciencias, Pontificia Universidad Católica del Perú, Lima, Peru
- 92 Sezione INFN, Trieste, Italy
- 93 Sezione INFN, Padova, Italy
- 94 Sezione INFN, Turin, Italy
- 95 Sezione INFN, Rome, Italy
- 96 Sezione INFN, Cagliari, Italy
- 97 Sezione INFN, Bologna, Italy
- 98 Sezione INFN, Bari, Italy
- 99 Sezione INFN, Catania, Italy
- 100 Soltan Institute for Nuclear Studies, Warsaw, Poland
- 101 Nuclear Physics Group, STFC Daresbury Laboratory, Daresbury, United Kingdom
- 102 SUBATECH, Ecole des Mines de Nantes, Université de Nantes, CNRS-IN2P3, Nantes, France
- 103 Technical University of Split FESB, Split, Croatia
- 104 The Henryk Niewodniczanski Institute of Nuclear Physics, Polish Academy of Sciences, Cracow, Poland
- 105 The University of Texas at Austin, Physics Department, Austin, TX, United States
- 106 Universidad Autónoma de Sinaloa, Culiacán, Mexico
- 107 Universidade de São Paulo (USP), São Paulo, Brazil
- 108 Universidade Estadual de Campinas (UNICAMP), Campinas, Brazil
- 109 Université de Lyon, Université Lyon 1, CNRS/IN2P3, IPN-Lyon, Villeurbanne, France
- 110 University of Houston, Houston, Texas, United States
- 111 University of Tennessee, Knoxville, Tennessee, United States
- 112 University of Tokyo, Tokyo, Japan
- 113 University of Tsukuba, Tsukuba, Japan
- 114 Eberhard Karls Universität Tübingen, Tübingen, Germany
- 115 Variable Energy Cyclotron Centre, Kolkata, India
- 116 V. Fock Institute for Physics, St. Petersburg State University, St. Petersburg, Russia
- 117 Warsaw University of Technology, Warsaw, Poland
- 118 Wayne State University, Detroit, Michigan, United States
- 119 Yale University, New Haven, Connecticut, United States
- 120 Yerevan Physics Institute, Yerevan, Armenia
- 121 Yildiz Technical University, Istanbul, Turkey
- 122 Yonsei University, Seoul, South Korea
- 123 Zentrum für Technologietransfer und Telekommunikation (ZTT), Fachhochschule Worms, Worms, Germany